View Online / Journal Homepage / Table of Contents for this issue

Encapsulated transition metal catalysts comprising peripheral Zn(II)salen building blocks: template-controlled reactivity and selectivity in hydroformylation catalysis†

Arjan W. Kleij,[a] Martin Lutz,[b] Anthony L. Spek,[b] Piet W. N. M. van Leeuwen[a] and Joost N. H. Reek*[a]

Received (in Cambridge, UK) 14th March 2005, Accepted 13th May 2005
First published as an Advance Article on the web 10th June 2005
DOI: 10.1039/b503708e

Published on 10 June 2005 on http://pubs.rsc.org | doi:10.1039/B503708E
Downloaded by University of Virginia on 27 July 2012

Encapsulated phosphane ligands can be easily constructed through coordinative interactions between Zn(II)–salphen complexes and pyridylphosphane templates; the template has a pronounced impact on the catalyst structure and consequently on the performance in the hydroformylation of 1-octene.

Coordination chemistry constitutes a highly useful tool in supramolecular chemistry,[1] and various assemblies with appealing 3D-structures based on various building blocks such as calixarene/resorcinarene,[2] porphyrin,[3] or other components[4] have been reported. Molecular capsules represent an interesting class of assemblies since the internal cavities can accommodate small organic molecules. Chemical conversions applied within these cavities is particularly fascinating, and molecular encapsulation has ambiguously opened up new opportunities to control reactivity and selectivity behavior.[5]

Previously, we have introduced a templated approach towards encapsulated homogeneous catalysts using Zn(II)porphyrins. These supramolecular assemblies comprised highly selective Zn(II)–pyridine coordinative binding motifs.[6] The variation of the porphyrin building block in the supramolecular P-assembly using tris(*meta*-pyridyl)phosphane as template was effectively used to steer the reactivity and selectivity of the catalyst.[6a,6b] Here, we introduce a new class of encapsulated catalysts based on the assembly of different pyridyl–phosphane templates and Zn(II)–salphen complexes through selective pyridine–Zn coordination that has a higher stability constant than the porphyrin analogue.[7] The structural features of these Zn–salphen building blocks can be altered easily and therefore fine-tuning of the desired supramolecular assemblies is more straightforward as compared to the porphyrin-based assemblies. More importantly, we will demonstrate that the pyridylphosphane template structure (**P2** *vs.* **P3**, Scheme 1) has a large influence on the structural features of the formed assembly and consequently on the catalytic performance in the hydroformylation of 1-octene.

As a model study, the interaction between diphenyl 4-pyridylphosphane (**P1**) and Zn(II)–salphen **1** was studied by NMR and UV-vis spectroscopy (Scheme 1). UV-vis titration experiments in toluene revealed a very high association constant for the assembly **1**·**P1** (K_{ass} = 4.0 × 10^5 M^{-1}), whereas PPh_3 showed no measurable association to **1**. This implies that the phosphorus centre in **1**·**P1** is still available for selective coordination to other metal fragments. Importantly, in contrast to similar porphyrin assemblies the Zn–pyridine interaction is still of substantial magnitude in more polar solvents, and NMR-titrations in d_6-acetone gave a binding constant of K_{ass} = 2.3 × 10^3 M^{-1} for **1**·**P1**. NMR analysis (d_6-acetone) revealed a significant up-field shift ($\Delta\delta$ = 0.26 ppm) for the pyr-H_{ortho} proton of **P1** upon complexation to **2**. The $^{31}P\{^1H\}$ resonance shifted only slightly ($\Delta\delta$ = 1.50 ppm), which supported a selective Zn–pyridine coordination. Single and sharp resonance patterns were observed, which corroborate fast exchange processes on the NMR time scale.

Higher-order assemblies were created with pyridylphosphanes **P2** and **P3** (Scheme 1). UV-vis titration and NMR spectroscopic experiments with **P2**/**P3** and complex **1** supported the formation of the 3 : 1 assemblies (**1**)$_3$·**P2** and (**1**)$_3$·**P3**. We were unable to obtain reliable association constants for these assemblies, but from the titration curves we can estimate that they are in the same range as that of **1**·**P1**. The ^1H NMR spectra (d_6-acetone) for (**1**)$_3$·**P2** displayed a similar up-field shift for the pyr-H_{ortho} protons ($\Delta\delta$ = 0.29 ppm) as compared to assembly **1**·**P1**, and a

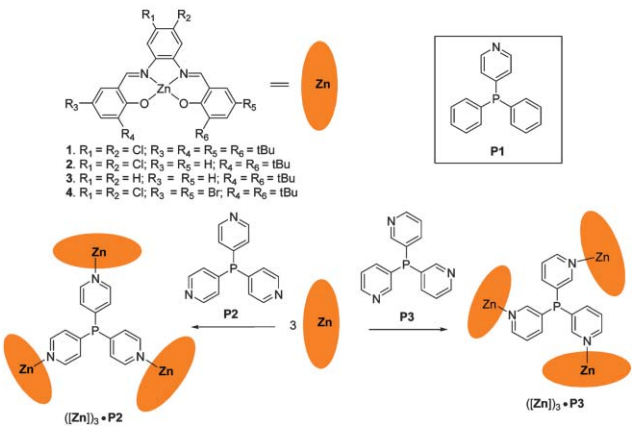

Scheme 1 Assembly formation between pyridylphosphanes **P1**–**P3** and Zn–salphen complexes **1**–**4** and schematic drawing of the 3 : 1 assemblies ([Zn])$_3$·**P2** and ([Zn])$_3$·**P3**.

[a]*Van't Hoff Institute for Molecular Sciences, University of Amsterdam, Nieuwe Achtergracht 166, 1018 WV, Amsterdam, The Netherlands. E-mail: reek@science.uva.nl; Fax: +3120-5256422; Tel: +3120-5256437*
[b]*Department of Crystal and Structural Chemistry, Bijvoet Center for Biomolecular Research, Utrecht University, Padualaan 8, 3584 CH, Utrecht, The Netherlands. Fax: +3130-2533940; Tel: +3130-2532538*

† Electronic supplementary information (ESI) available: Titration curves, experimental details, molecular modelling studies and displacement ellipsoid plot for assembly (**1**)$_3$·**P2**. See http://www.rsc.org/suppdata/cc/b5/b503708e/

Published on 10 June 2005 on http://pubs.rsc.org | doi:10.1039/B503708E
Downloaded by University of Virginia on 27 July 2012

comparable, relatively small shift of the $^{31}P\{^{1}H\}$ resonance ($\Delta\delta$ = 1.62 ppm). Likewise, the observed changes for $(\mathbf{1})_3\cdot\mathbf{P3}$ were rather similar (CD_2Cl_2, $\Delta\delta$(pyr-H_{ortho}) = 0.38 and 0.33 ppm, $\Delta\delta$ $^{31}P\{^{1}H\}$ NMR = 0.56 ppm). Crystals of assembly $(\mathbf{2})_3\cdot\mathbf{P2}$ suitable for X-ray analysis[8] were obtained from CH_2Cl_2–CH_3CN and the structure is visualised in Fig. 1.‡ Although the assembly is rather bulky, the phosphorus centre is not completely encapsulated. Interestingly, one of the three salphen units has a different orientation, with the chloro atoms pointing in another direction. Obviously, such a preferred frozen arrangement in the solid state is lost in solution as a result of the dynamic behavior of the Zn–N_{pyr} interaction. The unit cell of $(\mathbf{2})_3\cdot\mathbf{P2}$ clearly illustrates that the two phosphane centres are proximally orientated (the shortest P···P distance is 7.0965(16) Å, see Fig. 2). Also, the Zn(II)-complex **2** and phosphane template **P2** are preorganised and present in a 6 : 2 ratio suggesting that the formation of a diphosphane metal complex should be feasible.

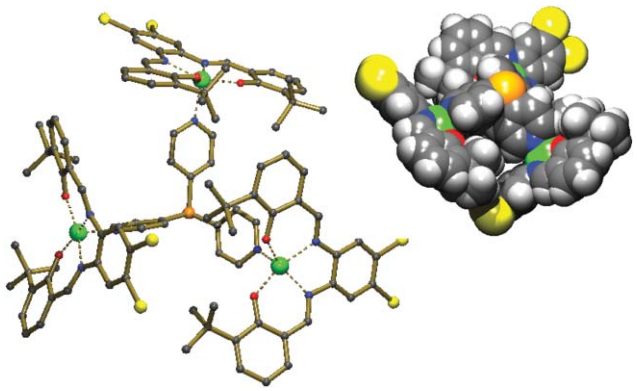

Fig. 1 Molecular structure of $(\mathbf{2})_3\cdot\mathbf{P2}$ in the crystal shown from different angles. Co-crystallized acetonitrile solvent molecules are omitted for clarity. For numbering scheme and selected distances see supporting information.†

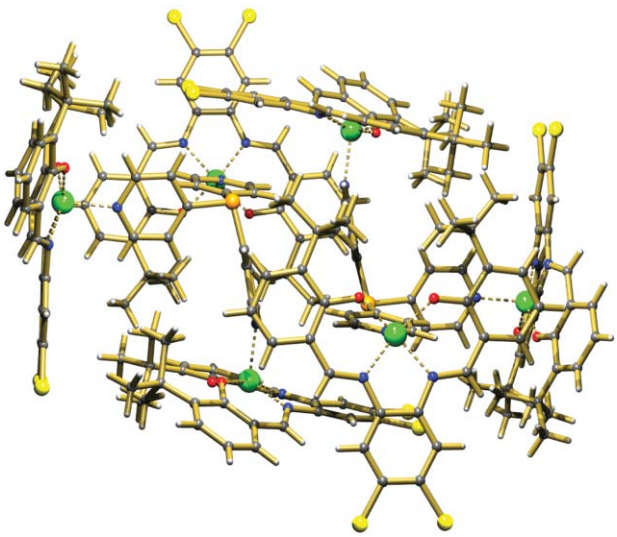

Fig. 2 A plot showing the crystallographic unit cell containing two template ligands (**P2**) encapsulated by six salphen building blocks (**2** : **P2** = 6 : 2). The orange atoms represent the phosphane centres (green = Zn, blue = N, red = O, gray = C, yellow = Cl).

Molecular modelling (PM3 calculations, see supporting information†) clearly shows the effect of the template on the encapsulation efficiency of the phosphorus ligand. A much more accessible phosphorus centre is available in assembly $(\mathbf{2})_3\cdot\mathbf{P2}$ as compared to $(\mathbf{2})_3\cdot\mathbf{P3}$. Consequently, the difference in steric demands upon complexation to a metal precursor between **P2** and **P3** should lead to preferential mono-phosphane or diphosphane metal complexes, which will show different catalytic properties.[6b]

A 2 : 1 mixture of $(\mathbf{1})_3\cdot\mathbf{P3}$ and $Rh(CO)_2(acac)$ in CD_2Cl_2 was examined by $^{31}P\{^{1}H\}$ NMR and showed a doublet at δ = 43.3 (^{1}J[Rh–P] = 182 Hz) and a singlet line at −20.9 ppm (*i.e.*, free encapsulated $(\mathbf{1})_3\cdot\mathbf{P3}$)) in an approximate 1 : 1 integral ratio. This result supports the formation of a mono-phosphane ligated Rh-species, as expected on the basis of the modelling results. Although NMR studies with $(\mathbf{1})_3\cdot\mathbf{P2}$ revealed the presence of two diphosphane metal species with resonances at δ = 31.4 ppm (^{1}J[Rh–P] = 147 Hz) and δ = 30.3 ppm (^{1}J[Rh–P] = 139 Hz), also other species could be observed.[9] Mono- and diphosphane assignments were corroborated by separate NMR experiments (CD_2Cl_2) with PPh_3 as ligand at 1 : 1 (δ = 50.4 ppm, ^{1}J[Rh–P] = 178 Hz) and 2 : 1 P : Rh ratios (δ = 33.3 ppm, ^{1}J[Rh–P] = 141 Hz).

In order to authenticate that diphosphane species based on **P2** are feasible, NMR experiments with (COD)$PtCl_2$ were carried out. First, a 1 : 2 mixture of this salt with **P2** was analysed showing the formation of the bis-phosphane, *cis*-complex $PtCl_2(\mathbf{P2})_2$ with ^{1}J(Pt–P) = 3648 Hz. Subsequent addition of 6 equivalents of **1** to this mixture gave rise to the exclusive formation of the assembly $PtCl_2[(\mathbf{1})_3\cdot\mathbf{P2}]_2$ with ^{1}J(Pt–P) = 2820 Hz, and no free phosphane $(\mathbf{1})_3\cdot\mathbf{P2}$ was observed. The coupling constant of 2820 Hz strongly points to the presence of a *trans*-complex. Obviously, the steric crowding induced by the encapsulation provokes this *cis*-to-*trans* isomerism.

The encapsulated phosphanes were used as ligands in the rhodium-catalysed hydroformylation of 1-octene (20 bar syngas, 1 : 1 CO–H_2) at ambient temperature (see Table 1).[10] Entries 1–3 show that the monodentate ligands PPh_3, **P2** and **P3** give rise to the same expected selectivity and that the use of **P2**, the ligand with the 4-pyridyl substituents, results in higher conversion. This is consistent with our previous results[11] and the higher reactivity is explained by the electron-withdrawing effect of the 4-pyridyl

Table 1 Hydroformylation of 1-octene in toluene with ligand assemblies based on **P2** or **P3** leading to linear (**L**) or branched (**B**) aldehyde products. **IS** denotes isomerised internal olefin species[a]

Entry	Ligand	Conversion (%)	IS (%)[b]	L/B	L (%)	B (%)
1	$\mathbf{PPh_3}$	27	1.0	2.6	72	28
2	**P2**	67	1.4	2.7	73	27
3	**P3**	31	2.4	2.3	70	30
4	$(\mathbf{1})_3\cdot\mathbf{P2}$	27	5.1	2.2	69	31
5	$(\mathbf{3})_3\cdot\mathbf{P2}$	15	6.1	2.7	73	27
6	$(\mathbf{1})_3\cdot\mathbf{P3}$	97	1.1	1.4	59	41
7	$(\mathbf{2})_3\cdot\mathbf{P3}$	97	2.5	1.0	49	51
8	$(\mathbf{3})_3\cdot\mathbf{P3}$	97	1.6	1.2	56	44
9	$(\mathbf{4})_3\cdot\mathbf{P3}$	97	2.4	0.8	45	55

[a] Reagents and conditions: $Rh(acac)(CO)_2$ = 0.7 mM in toluene, pressure = 20 bar (CO : H_2 = 1 : 1), 1-octene : rhodium = 1052 : 1, [P] = 6.4 mM, reaction conditions: 65 h, 25 °C. Reactions were performed *in duplo*. [b] Total amount of isomerisation based on converted 1-octene.

 This journal is © The Royal Society of Chemistry 2005

View Online

Published on 10 June 2005 on http://pubs.rsc.org | doi:10.1039/B503708E
Downloaded by University of Virginia on 27 July 2012

groups. The catalytic data show a number of interesting differences between the use of ligand assemblies based on **P2** and **P3**. The assemblies based on **P2** give rise to much slower rhodium catalysts as compared to the parent phosphane **P2**, though the selectivity characteristics of typical diphosphane-ligated hydroformylation catalysts are preserved (*cf.* entries 1–5). These results clearly point to the presence of a diphosphane species during catalysis. The lower activity of the catalysts with the **P2**-assembly ligands as compared to parent **P2** is ascribed to the steric impact of the Zn(II)–salphen complexes in the 'second coordination sphere' of the rhodium metal centre. In contrast, the catalysts derived from the **P3**-assemblies show much *higher* activity (at least a 4-fold increase) than their non-assembled parent phosphane **P3**, PPh_3 (entries 1 and 3 *vs.* 6–9) and the **P2**-based assemblies (entries 4–5). In addition, a different selectivity behavior is noted using these **P3**-assemblies, and in general higher amounts of branched aldehyde (**B**) (up to 55%, entry 9) are formed. These results agree with the presence of a mono-phosphane rhodium catalyst during catalysis.[6a,b,12] Clearly, the encapsulation of phosphane template **P3** upon addition of Zn(II)–salphen building blocks is far more effective than for template **P2**.

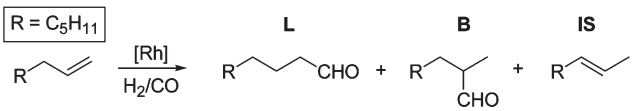

In summary, we have demonstrated that Zn(II)–salphen complexes are excellent building blocks for the construction of catalytically active supramolecular assemblies based on coordinative N_{pyr}–Zn patterns. More importantly, small differences in the phosphane template structure can be used to modify the catalytic properties of the metal centre upon complexation to these salphen structures and fine-tuning is viable through a proper choice of the supramolecular building blocks (*i.e.*, salphen and/or porphyrin complexes). Particularly in the case of **P3**, encapsulation results in effective shielding of the phosphorus atom. From the X-ray structure it is clear that the assemblies based on **P2** are sufficiently open to allow the formation of a bis-phosphane metal complex. We have successfully used this template effect in the hydroformylation of 1-octene and a substantial difference in the regioselectivity and activity was observed between the use of **P2**- and **P3**-assemblies. This can be attributed to the structural difference of the intermediate Rh(I)-species (diphosphane ligation for **P2** *vs.* mono-phosphane ligation for **P3**), which is supported by the NMR spectroscopic, X-ray crystallographic and modelling studies. Currently, our research program is focused on the full exploitation of these new phosphine assemblies to make extended catalyst libraries and the optimisation of various organic transformations.

Notes and references

‡ Crystal structure determination: Structure $(\mathbf{2})_3{\cdot}\mathbf{P2}$: $C_{99}H_{96}Cl_6N_9O_6PZn_3{\cdot}5CH_3CN$, FW = 2152.90, yellow needle, 0.36 × 0.12 × 0.09 mm^3, triclinic, $P\bar{1}$ (No. 2), a = 14.4818(3), b = 17.0579(3), c = 23.2334(4) Å, α = 78.2385(6), β = 87.6536(6), γ = 71.2122(9)°, V = 5317.55(17) $Å^3$, Z = 2, ρ = 1.345 g cm^{-3}, μ = 0.90 mm^{-1}, 57108 measured reflections, 15149 unique reflections (R_{int} = 0.082). Absorption correction based on multiple measured reflections (correction range 0.83–0.92). Non H-atoms were refined freely with anisotropic displacement parameters. H-atoms were introduced in calculated positions. H-atoms of the acetonitrile molecules were kept fixed during refinement. All other H-atoms were refined as rigid groups. 1270 refined parameters; no restraints. R ($I > 2\sigma(I)$): $R1$ = 0.0421, w$R2$ = 0.0794. R (all data): $R1$ = 0.0857, w$R2$ = 0.0958, S = 1.031. Residual electron density between −0.33 and 0.40 e $Å^{-3}$. CCDC 251478. See http://www.rsc.org/suppdata/cc/b5/b503708e/ for crystallographic data in CIF or other electronic format.

1 (*a*) J. L. Sessler, B. Wang, S. L. Springs and C. T. Brown, in *Comprehensive Supramolecular Chemistry*, ed. Y. Murakami, Pergamon, Oxford, 1996; (*b*) J.-M. Lehn, *Supramolecular Chemistry*, Weinheim, 1995; (*c*) S. Leininger, B. Olenyuk and P. J. Stang, *Chem. Rev.*, 2000, **100**, 853.

2 (*a*) F. Fochi, P. Jacopozzi, E. Wegelius, K. Rissanen, P. Cozzini, E. Marastoni, E. Fisicaro, P. Manini, R. Fokkens and E. Dalcanale, *J. Am. Chem. Soc.*, 2001, **123**, 7539; (*b*) A. M. Rincón, P. Prados and J. de Mendoza, *J. Am. Chem. Soc.*, 2001, **123**, 3493; (*c*) J. de Mendoza, *Chem. Eur. J.*, 1998, **4**, 1373; (*d*) K. D. Shimizu and J. Rebek, *Proc. Natl. Acad. Sci. USA*, 1995, **92**, 12403; (*e*) L. R. MacGillivray and J. L. Atwood, *Nature*, 1997, **289**, 469.

3 (*a*) L. G. Mackay, R. S. Wylie and J. K. M. Sanders, *J. Am. Chem. Soc.*, 1994, **116**, 3141; (*b*) C. M. Drain and J.-M. Lehn, *J. Chem. Soc., Chem. Commun.*, 1994, 2313; (*c*) P. J. Stang, J. Fan and B. Olenyuk, *Chem. Commun.*, 1997, 1453; (*d*) K. Funatsu, T. Imamura, A. Ichimura and Y. Sasaki, *Inorg. Chem.*, 1998, **37**, 4986; (*e*) A. Okumura, K. Funatsu, Y. Sasaki and T. Imamura, *Chem. Lett.*, 1999, 779; (*f*) W. T. S. Huck, A. Rohrer, A. T. Anilkumar, R. H. Fokkens, N. M. M. Nibbering, F. C. J. M. van Veggel and D. N. Reinhoudt, *New J. Chem.*, 1998, 165; (*g*) C. A. Hunter and L. D. Sarson, *Angew. Chem., Int. Ed.*, 1994, **33**, 2313.

4 (*a*) M. Fujita, N. Fujita, K. Ogura and K. Yamaguchi, *Nature*, 1999, **400**, 52; (*b*) L. R. MacGillivray and J. L. Atwood, *Angew. Chem., Int. Ed.*, 1999, **38**, 1018; (*c*) M. Tominaga, K. Suzuki, M. Kawano, T. Kusukawa, T. Ozeki, S. Sakamoto, K. Yamaguchi and M. Fujita, *Angew. Chem., Int. Ed.*, 2004, **43**, 5621; (*d*) T. Beissel, R. E. Power and K. N. Raymond, *Angew. Chem., Int. Ed. Engl.*, 1996, **35**, 1084; (*e*) B. Olenyuk, J. A. Whiteford, A. Fechtenkotter and P. J. Stang, *Nature*, 1999, **398**, 796.

5 (*a*) J. Kang and J. Rebek, *Nature*, 1997, **385**, 50–52; (*b*) M. L. Merlau, M. P. Mejia, S. T. Nguyen and J. T. Hupp, *Angew. Chem., Int. Ed.*, 2001, **40**, 4239; (*c*) D. H. Leung, D. Fiedler, R. G. Bergman and K. N. Raymond, *Angew. Chem., Int. Ed.*, 2004, **43**, 963–966; (*d*) M. Yoshizawa, Y. Takeyama, T. Kusukawa and M. Fujita, *Angew. Chem., Int. Ed.*, 2002, **41**, 1347; (*e*) M. Ziegler, J. L. Brumaghim and K. N. Raymond, *Angew. Chem., Int. Ed.*, 2000, **39**, 4119; (*f*) A. Lützen, *Angew. Chem., Int. Ed.*, 2005, **44**, 1000; (*g*) D. Fiedler, D. H. Leung, R. G. Bergman and K. N. Raymond, *Acc. Chem. Res.*, 2005, **38**, 351.

6 (*a*) V. F. Slagt, P. J. C. Kamer, P. W. N. M. van Leeuwen and J. N. H. Reek, *J. Am. Chem. Soc.*, 2004, **126**, 1526; (*b*) V. F. Slagt, J. N. H. Reek, P. J. C. Kamer and P. W. N. M. van Leeuwen, *Angew. Chem., Int. Ed.*, 2001, **40**, 4271; (*c*) V. F. Slagt, M. Röder, P. J. C. Kamer, P. W. N. M. van Leeuwen and J. N. H. Reek, *J. Am. Chem. Soc.*, 2004, **126**, 4056; (*d*) V. F. Slagt, P. W. N. M. van Leeuwen and J. N. H. Reek, *Chem. Commun.*, 2003, 2474; (*e*) V. F. Slagt, P. W. N. M. van Leeuwen and J. N. H. Reek, *Angew. Chem., Int. Ed.*, 2003, **42**, 5619.

7 A. W. Kleij, M. Kuil, D. M. Tooke, M. Lutz, A. L. Spek and J. N. H. Reek, *Chem. Eur. J.*, 2005, DOI: 10.2002/chem.200500227.

8 The crystallisation of assemblies of Zn–salphen complex **2** proved to be easier than **1**.

9 When **2** was used as Zn(II)–salpen complex in these NMR experiments, the same species were observed in the $^{31}P\{^1H\}$ NMR spectrum. Non-exclusive formation of a diphosphane species based on this Rh-precursor can be interpreted as the influence of the *cis*-coordinating mode of the bidentate acac-ligand, which effectively blocks a *trans*-spanning of the two phosphane ligands through isomerisation.

10 Under the conditions applied the salphen building blocks are not affected, which was confirmed in a separate control experiment.

11 A. Buhling, P. C. J. Kamer and P. W. N. M. van Leeuwen, *J. Mol. Catal.*, **98**, 69.

12 (*a*) A. van Rooy, E. N. Orij, P. C. J. Kamer and P. W. N. M. van Leeuwen, *Organometallics*, 1995, **14**, 34; (*b*) P. W. N. M. van Leeuwen and C. F. Roobeek, *J. Organomet. Chem.*, 1983, **258**, 343; (*c*) B. Breit and E. Fuchs, *Chem. Commun.*, 2004, 694; (*d*) B. Breit, R. Winde, T. Mackewitz, R. Paciello and K. Harms, *Chem. Eur. J.*, 2001, **7**, 3106.